SYNTHESIS OF ZINC FERRITE NANOPOWDERS IN AN RF THERMAL PLASMA

I. Mohai[1], J. Szépvölgyi[1], J. Gubicza[2]

[1]Research Laboratory of Materials and Environmental Chemistry, Chemical Research Center, Hungarian Academy of Sciences, P.O.B. 17, Budapest, H-1525, Hungary
[2]Department of General Physics, Eötvös University, P.O.B. 32, Budapest, H-1518, Hungary

Abstract

Nanosized zinc ferrite spinel powders of various compositions were produced in an RF thermal plasma from oxide mixtures and from co-precipitated hydroxides. The products were characterised for bulk chemical (ICP-AES), and phase composition (XRD). In spite of the short residence time of the reagents in the plasma reactor considerable extent of spinel formation was achieved. Magnetization and Curie point measurements indicated that the spinel phases exhibited ferrimagnetic behaviour. Ferrites synthetized in the RF plasma reactor were compared to that produced by the conventional ceramic route.

1. Introduction

The spinel ferrites contain a close-packed cubic structure of oxygen ions in which tetrahedral (A) an octahedral (B) interstitial sites are occupied by cations [1]. Zinc ferrite belongs to the class of normal spinels which presumably have a cation distribution of $(Zn^{2+})_A((Fe^{3+})_2)_B(O^{2-})_4$. It is paramagnetic at room temperature. However, in special synthesis conditions (e.g. co-precipitation [2], rapid quenching [3] and mechanochemical activation [4]) some Fe^{3+} ions may occupy tetrahedral, as well as octahedral sites forming the inverse spinel structure. The strong superexchange interaction among these sites results in an unusually high magnetisation as compared to normal spinels [3]. A direct correlation was found between the particle size and the saturation magnetisation: the finer the particles were, the more saturation magnetisation could be measured [5,6]. The relatively high magnetisation of pure Fe_3O_4 can be further increased by Zn substitution and the highest saturation magnetisation ever found in spinel ferrites can be measured for zinc ferrous ferrites ($Zn_xFe_{3-x}O_4$ where $x \leq 0.5$) [7].

Radiofrequency thermal plasmas offer unique advantages for the synthesis of special ceramic powders due to the high temperatures and energy densities in these systems. In addition, a high temperature gradient exists between the hot plasma flame and the surrounding gas phase. The resulting rapid quenching rate is favourable for producing fine particles with unstable structures in thermodynamic terms. In this paper results on the thermal plasma synthesis of zinc ferrites and zinc ferrous ferrites are presented.

2. Experimental

Precursors for the synthesis of $Zn_XFe_{3-X}O_4$ (0<x≤1) were prepared by two methods:

- Fe_2O_3 and ZnO powders of analytical grade were thoroughly mixed in an agate mortar in a molar ratio of 2:1.
- $Fe(NO_3)_3 \cdot 6H_2O$ and ZnO, with Fe:Zn = 2:1 and 6:1 molar ratio, were dissolved in deionised water. The pH of the solution was set to 8 by adding NH_4OH solution. The precipitated hydroxides were washed with deionized water, filtered and dried at 80ºC.

The precursors were treated in a laboratory scale RF thermal plasma reactor (Linn, 27 MHz, 1-7 kW) connected to an air cooled, two-stage powder collector. Argon was used as the central plasma gas (7 l·min^{-1}) and as the sheath gas (19 l·min^{-1}), as well. The powder was injected continuously into the plasma tail flame region by carrier gas (argon or air) passed through a fluidised and vibrated powder-bed. Products deposited on the reactor wall (Samples R) and in the powder collector (Samples C) were collected and analysed separately. To make a comparison between ferrites prepared in the plasma reactor with those obtained by the conventional ceramic processing the oxide mixture and the co-precipitated hydroxides were calcined in air at 900ºC for 6h, as well.

The bulk chemical composition of dissolved samples was analysed by ICP-AES (Labtest PSX75). Crystalline phases were identified by X-ray diffraction (XRD) using a Philips Xpert diffractometer and CuKα radiation (λ=0.15418 nm). The lattice parameters (a) of the crystalline phases were determined from the positions of diffraction peaks. The mean grain-size was calculated from the full widths at the half maximum (FWHM) of the most intensive diffraction profiles according to the Scherrer's equation. Magnetisation measurements were performed using a SQUID-magnetometer. The Curie point of the samples was determined by measuring mass changes against the temperature (Perkin-Elmer TGS-2 thermobalance) applying a constant magnetic field.

3. Results and discussion

Conditions of sample preparation and results of XRD analysis are collected in Table 1. The X-ray diffractograms are shown in Fig. 1 (for Samples 1 and 2C), in Fig. 2 (for Samples 3, 4R and 4C) and in Fig. 3 (for Samples 5, 6R, 6C, 7R, 7C). The XRD pattern of the heat-treated oxide mixture (900ºC, 6h) shows the formation of the spinel phase (Fig 1. Sample 1.). Reflections of Fe_2O_3 and ZnO almost completely disappeared. The calculated lattice parameter (a) is equal to that of $ZnFe_2O_4$ within the limits of the experimental error (Table 1, Sample 1). Contrary to the "conventional" synthesis, the plasma treatment of the oxide mixture resulted in the formation of magnetite (Fe_3O_4) with the incorporation of a small amount of Zn only (Fig. 1. Sample 2C). The spinel composition was estimated by assuming the increase of lattice parameter due to Zn incorporation to be proportional with the Zn concentration. The calculated composition indicated the presence of about 0.1 mol of Zn in the spinel structure ($Zn_{0.1}Fe_{2.9}O_4$). The Particular ferrite probably formed through the condensation of oxide vapours. The small mean size of spinel grains (D = 34 nm) supports this assumption. During the plasma treatment of the oxide precursor the spinel formation was not complete. In addition to the unreacted ZnO a high amount of Fe_2O_3 was found in the product, as well. We suppose that in spite of the high specific energy (4 kWh/g oxide) the

larger, aggregated grains could not decompose and evaporate because of their short residence time in the hot plasma region.

Table 1 Methods of sample preparation and results of XRD measurements. Plasma treated samples were collected from the reactor (R) and the from the cyclone (C). Composition of the spinel phase was estimated from the lattice parameter (a). The mean grain size (D) was calculated from the FWHM of XRD profiles.

Sample No.	Precursor	Fe:Zn[a]	Method	Spinel phase			Other phases[b]	
				a (Å)	Composition	D (nm)	H/S	Z/S
1	Oxide	2:1	900°C, 6h	8.439	$ZnFe_2O_4$	100	0	0
2C	Oxide	2:1	Plasma (Ar)	8.400	$Zn_{0.1}Fe_{2.9}O_4$	34	0.49	0.55
3	Hydroxide	2:1	900°C, 6h	8.441	$ZnFe_2O_4$	119	0.05	0
4R	Hydroxide	2:1	Plasma (Ar+air)	8.438	$ZnFe_2O_4$	49	0.05	0.06
4C	Hydroxide	2:1	Plasma (Ar+air)	$\begin{cases} 8.438 \\ 8.392 \end{cases}$	$ZnFe_2O_4$ / Fe_3O_4	50 / 57	0.05	0.08
5	Hydroxide	6:1	900°C, 6h	8.439	$ZnFe_2O_4$	65	0.89	0
6R	Hydroxide	6:1	Plasma (Ar)	8.414	$Zn_{0.4}Fe_{2.6}O_4$	48	0.06	0.09
6C	Hydroxide	6:1	Plasma (Ar)	8.415	$Zn_{0.4}Fe_{2.6}O_4$	42	0	0.1
7R	Hydroxide	6:1	Plasma (Ar+air)	8.424	$Zn_{0.6}Fe_{2.4}O_4$	25	0.7	0
7C	Hydroxide	6:1	Plasma (Ar+air)	$\begin{cases} 8.438 \\ 8.393 \end{cases}$	$ZnFe_2O_4$ / Fe_3O_4	47 / 62	0.17	0

[a] Molar ratio
[b] H: Fe_2O_3 (hematite), Z: ZnO (zincite). The most intense reflection are related to the most intense spinel (S) reflection.
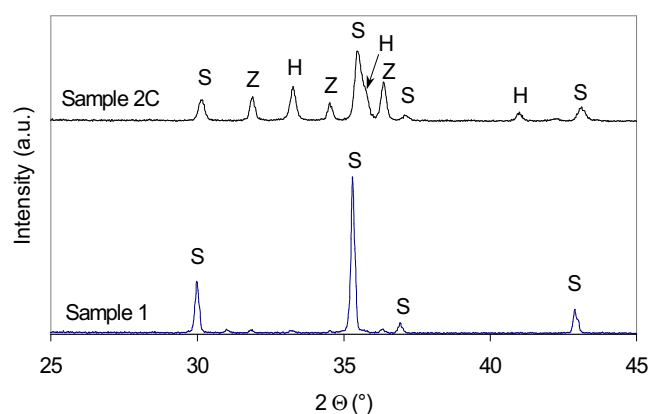

Fig. 1. X-ray diffractograms of samples prepared from Fe_2O_3+ZnO mixture by the conventional ceramic route (Sample 1) and by plasma treatment (Sample 2C). S: spinel, H: hematite (Fe_2O_3), Z: zincite (ZnO)

Extent of spinel formation from the Fe:Zn=2:1 hydroxide precursor was practically as high in the plasma treated samples as in the sample calcined at 900°C for 6h (Fig. 2.), although the specific energies applied in the case of hydroxide precursors were in the range of 0,3-0,5 kWh/g hydroxide (which is about one tenth as compared to the specific energy applied in the case of oxide precursor). Sample collected from the reactor wall (Sample 4R) differed from the sample deposited in the powder collector (Sample 4C) both in chemical and phase compositions. Iron and zinc content of Sample 4R (Fe=46.4, Zn=26.7 w/w%) was actually equal to the theoretical composition of $ZnFe_2O_4$.

However, in Sample 4C the iron content increased and the zinc content decreased (Fe=50.5% and Zn=22.9%) as compared to Sample 4R. Phase composition of relevant samples supported the results of chemical analysis: in Sample 4C the diffraction peaks of the spinel phase could be deconvoluted to two components; $ZnFe_2O_4$ (a=8.438 Å) and Fe_3O_4 (a:8.392 Å), respectively. Such significant differences of chemical and phase compositions in the same experiment indicate different formation mechanism. We suppose that in case of samples R the solid phase reaction between the oxides is the dominating process. This reaction can be relatively fast in the case of hydroxide precursor). Sample C collected from the powder collector was probably formed by condensation of vapours.

Treatment of the hydroxide-precursor (Fe:Zn = 6:1) in air at 900°C for 6h resulted in the formation of $ZnFe_2O_4$ phase (Table 1, Sample 5, Fig.3.). Formation of Fe_2O_3 could be
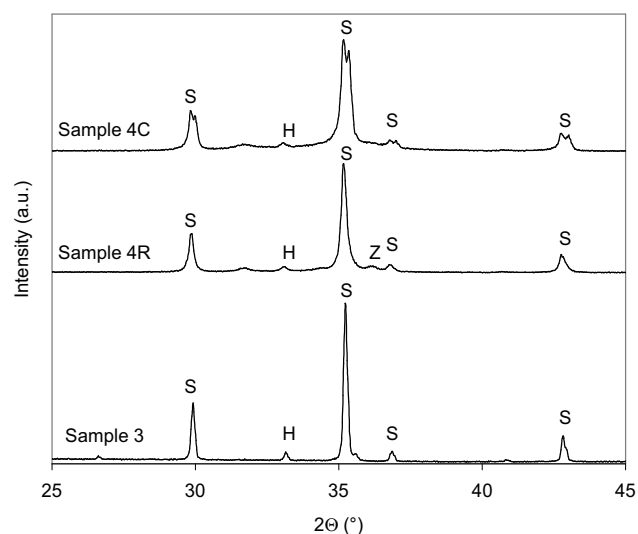

Fig. 2. X-ray diffractograms of samples prepared from hydroxide precursor (Fe:Zn=2:1) by the conventional ceramic route (Sample 3) and by plasma treatment (Samples 4R and 4C). S: spinel, H: hematite (Fe_2O_3), Z: zincite (ZnO)
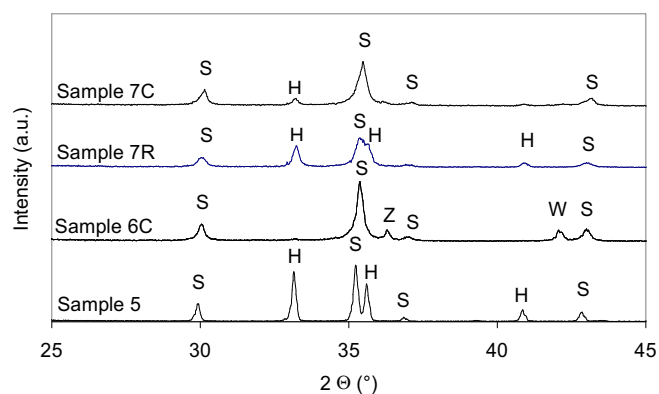

Fig. 3. X-ray diffractograms of samples prepared from hydroxide precursor (Fe:Zn=6:1) by the conventional ceramic route (Sample5) and by plasma treatment (Samples 6C, 7R and 7C). S: spinel, H: hematite (Fe_2O_3), Z: zincite (ZnO), W: wuestite (FeO).

attributed to the excess of iron. The composition of zinc ferrites could hardly be influenced using the conventional ceramic technique, unless the oxygen partial pressure is maintained in a proper range. However, the thermal plasma treatment of co-precipitated hydroxides in argon atmosphere resulted in a spinel phase with an estimated composition of $Zn_{0.4}Fe_{2.6}O_4$ (Samples 6R and 6C). Part of the Fe_2O_3 was reduced in these conditions and FeO (wuestite) was formed. The product contained some ZnO, as well. Spinel composition calculated from the cell parameter is very close to that calculated from the Fe:Zn ratio of the precursor ($Zn_{0.3}Fe_{2.7}O_4$) supposing a complete chemical transformation.

The role of oxygen in the spinel formation could be observed in Samples 7R and C. (Fig. 3.). In Sample 7R spinel phase was identified as $Zn_{0.6}Fe_{2.4}O_4$, which has a smaller Fe:Zn molar ratio (4:1) than the precorsor powder had (6:1). In sample 7C, like in the case of 4C, the diffraction peaks of the spinel phase could be deconvoluted to two components ($ZnFe_2O_4$, a=8.438 Å and Fe_3O_4, a:8.393 Å, respectively). Phases formed in the presence of air (Samples 4C and 7C) consisted of two separate spinel phases instead of forming a solid solution between $ZnFe_2O_4$ and Fe_3O_4 which is practically the case for zinc ferrous ferrites. Spinel formation from the Fe:Zn = 6:1 hydroxide precursor in the presence of air was not complete: rather high amount of Fe_2O_3 remained unreacted, especially in Sample 7R.
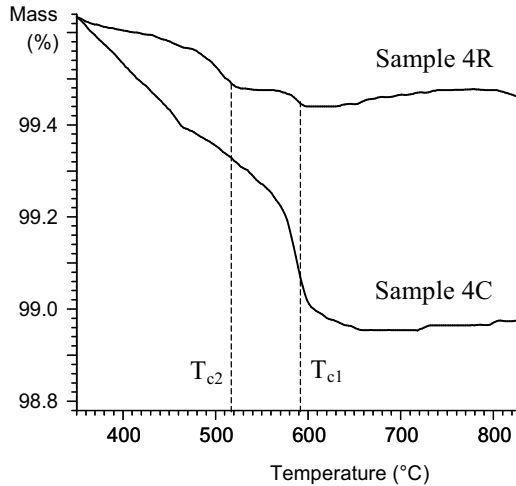

Fig. 4. Curie point measurements

The thermal analysis in a constant magnetic field is a very simple method for the magnetic characterization of materials. Well definied Curie points could be measured in plasma synthetized ferrites (Fig. 4.). T_{c1} at 590°C is present both in Sample 4R and C and can be attributed to the magnetite (Fe_3O_4) phase. The magnetite content of Sample 4R is probably very low, so it can not be identified by XRD analysis (Table 1.). However, in Sample 4R a different Curie point can be observed at about 530°C (T_{c2}). This temperature in not a characteristic one for ferrimagnetic substances. We may suppose, that particular Curie temperature indica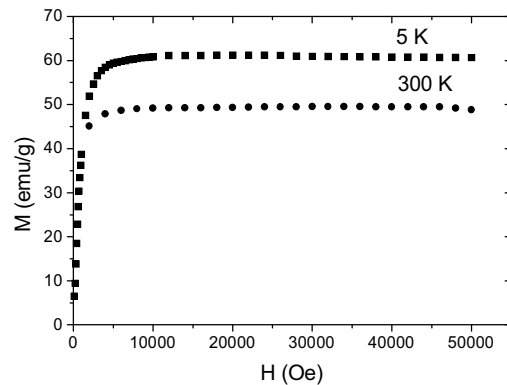tes the presence of ferrimagnetic zinc ferrite spinel. This measurement refers to the formation of inverse zinc ferrite spinels in thermal plasma conditions. In Sample 4C T_{c2} can not be measured because of the lower zinc ferrite content of the sample.

Magnetization measurements of Sample 2C indicated saturation magnetization of 61 emu/g at 5K and 50 emu/g at 300K (Fig. 5.). Semiquantitative analysis of the XRD measurements (taking into consideration chemical analysis data as well) revealed that mass ratio of the $Zn_{0.1}Fe_{2.9}O_4$ spinel phase to the unreacted Fe_2O_3 and ZnO phases was far less than 50%. This way the estimated saturation magnetization of the spinel phase can be above 100 emu/g. It is much higher than the saturation magnetization of magnetite (92 emu/g at 293K). This result is in good agreement with the data published recently by Brabers [7].

Fig. 5. Magnetization curves of Sample 2C

4. Conclusion

Nanosized spinel zinc ferrite phases of various compositions can be synthesised in an RF thermal plasma reactor in spite of the very short residence time of reagents in the hot plasma region. The iron and zinc containing precursors probably first atomise then vaporise near to the plasma flame. Spinels are forming during the condensation. This mechanism is supported by the fine (20-50 nm) particle size of powders produced. Conversion of the precursors in the plasma reactor was not complete, especially in the case of oxide precursor. Nearly the total amount of the hydroxide transformed into spinel phase. It suggests the importance of the grain size and the intimate mixing of precursors. Partial pressure of the oxygen can easily be adjusted in the plasma reactor. Thus, zinc ferrous ferrites can also be synthesised in these systems. Curie points of the plasma treated samples can be attributed to magnetite (T_c=590°C) and zinc ferrite (T_c=530°C), respectively. From the results of magnetization measurements a saturation magnetization of the $Zn_{0.1}Fe_{2.9}O_4$ spinel phase of more than 100 emu/g could be estimated.

References

[1]   B.D. Cullity, Introduction to Magnetic Materials, Addison-Werley, Reading, MA, 1972.
[2]   M.R. Anantharaman, S. Jagatheesan, K.A. Malini, S. Sindhu, A. Narayanasamy, C.N. Chinnasamy, J.P. Jacobs, S. Reine, K. Seshan, R.H.H. Smits, H.H. Brongersma, J. Magn. Magn. Mat. **189** (1998) 83.
[3]   K. Tanaka, M. Makita, Y. Shmizugawa, K. Hirao, N. Soga, J. Phys. Chem. Solids **59** (1998) 1611.
[4]   V. Šepelák, U. Steinike, D. Chr. Uecker, S. Wissmann, K. D. Becker, J. Solid State Chem. **135** (1998) 52.
[5]   T. Sato, K. Haneda, N. Seki, T. Iijima, Appl. Phys. A **50** (1990) 13.
[6]   T. Kamiyama, K. Haneda, T. Sato, S. Ikeda, H. Asano, Solid State Commun. **81** (1992) 563.
[7]   V.A.M. Brabers, J. Phys. IV. France **7** (1997) C1-223.